Neural oscillations track the maintenance and proceduralization of novel instructions

Oscillations in novel instructions implementation

Silvia Formica[a], Carlos González-García[a], Mehdi Senoussi[a], and Marcel Brass[a,b]

[a] Department of Experimental Psychology, Ghent University, Belgium

[b] School of Mind and Brain/Department of Psychology, Humboldt Universität zu Berlin, Germany

Ghent University

Faculty of Psychology and Educational Sciences

Department of Experimental Psychology

Henri Dunantlaan 2

B-9000 Gent

Corresponding author: Silvia Formica (silvia.formica@ugent.be)

1

Abstract

Humans are capable of flexibly converting symbolic instructions into novel behaviors. Previous evidence and theoretical models suggest that the implementation of a novel instruction requires the reformatting of its declarative content into an action-oriented code optimized for the execution of the instructed behavior. While neuroimaging research focused on identifying the brain areas involved in such a process, the temporal and electrophysiological mechanisms remain poorly understood. These mechanisms, however, can provide information about the specific cognitive processes that characterize the proceduralization of information. In the present study, we recorded EEG activity while we asked participants to either simply maintain declaratively the content of novel S-R mappings or to proactively prepare for their implementation. By means of time-frequency analyses, we isolated the oscillatory features specific to the proceduralization of instructions. Implementation of the instructed mappings elicited stronger theta activity over frontal electrodes and suppression in mu and beta activity over central electrodes. On the contrary, activity in the alpha band, which has been shown to track the attentional deployment to task-relevant items, showed no differences between tasks. Together, these results support the idea that proceduralization of information is characterized by specific component processes such as orchestrating complex task settings and configuring the motor system that are not observed when instructions are held in a declarative format.

Keywords

Highlights

- Frontal theta power is increased during instructions implementation

- Attentional orienting in WM is analogous across maintenance and implementation

- Instructions implementation involves motor recruitment

1. Introduction

One peculiar aspect of human cognitive flexibility involves the ability to convert complex symbolic instructions into novel behaviors, even in the absence of prior practice (Cole, Laurent, & Stocco, 2013). Recent experimental evidence and theoretical proposals have put forward a serial heuristic model in which instructions are first encoded and maintained in a declarative format before being transformed into an action-oriented format (i.e., procedural representation) that allows executing the instructed task (Brass, Liefooghe, Braem, & De Houwer, 2017). Neuropsychological and behavioral evidence supports a dissociation between 'knowing' the content of an instruction and 'doing' the instructed cognitive or motor action, suggesting that maintaining its declarative content is insufficient to implement the instructed task, and that additional procedural codes are needed for optimal performance (Bhandari & Duncan, 2014; Duncan, Emslie, Williams, Johnson, & Freer, 1996; Liefooghe, Wenke, & De Houwer, 2012; Milner, 1963; Wenke, Gaschler, Nattkemper, & Frensch, 2009). Such immediate reformatting seems to occur only when the instruction is prepared for implementation, and not when participants merely maintain the information in a declarative manner, without the intention to implement (Liefooghe et al., 2012).

A growing number of fMRI studies has primarily focused on revealing which brain regions support the implementation of novel task sets (Demanet et al., 2016; González-García, Arco, Palenciano, Ramírez, & Ruz, 2017; Hartstra, Kühn, Verguts, & Brass, 2011; Hartstra, Waszak, & Brass, 2012; Palenciano, González-García, Arco, & Ruz, 2019; Ruge & Wolfensteller, 2010) and, more recently, on characterizing implementation-specific neural representations (Bourguignon, Braem, Hartstra, De Houwer, & Brass, 2018;

4

71 González-García, Formica, Wisniewski, & Brass, 2019; Muhle-Karbe, Duncan, De

72 Baene, Mitchell, & Brass, 2017; Palenciano, González-García, Arco, Pessoa, & Ruz,

73 2019; Ruge, Schäfer, Zwosta, Mohr, & Wolfensteller, 2019). These results consistently

74 point towards a crucial role of frontoparietal regions, and in particular of the prefrontal

75 cortex (PFC). Similarly, they provide evidence for distinct neural mechanisms supporting

76 implementing versus memorizing novel instructions (Brass et al., 2017). However, it is

77 still not clear to what extent declaratively representing information and proceduralization

78 involve processes that overlap or differ qualitatively. Crucially, investigating the oscillatory

79 dynamics of instruction implementation would allow to decompose the specific spectral

80 components that are involved in proceduralizing S-R mappings into action-oriented

81 codes, and to provide insights on their temporal unfolding. This would increase our

82 understanding of the functional significance of such processes, complementing the

83 knowledge on localization and representational format provided by fMRI research.

84 Specifically, we reasoned that both declarative maintenance and proactive

85 proceduralization of novel instructions likely engage certain shared processes, such as

86 selective attention towards the instructed content, whereas differences in brain activity

87 should reflect the reformatting process that is specific to the implementation of the

88 instruction. On the one hand, changes in the attentional focus are revealed by activity in

89 the alpha frequency range (8 – 14 Hz) (Hari & Salmelin, 1997; Klimesch, Sauseng, &

90 Hanslmayr, 2007; Senoussi, Moreland, Busch, & Dugué, 2019; van Ede, 2017).

91 Modulations of posterior alpha band oscillations are a well-established mechanism

92 associated with endogenous orienting of spatial attention and suppressing competition

93 from distractors, allowing for the enhancement of task-relevant information (Bonnefond &

94   Jensen, 2012; Jensen & Mazaheri, 2010; Sauseng et al., 2005). A substantial body of

95   evidence reports decrease of alpha amplitude over posterior parietal regions contralateral

96   to the attended spatial location, indicating mechanisms of orienting attention both to

97   salient stimuli in the perceptual space and towards internally held representations

98   (Capilla, Schoffelen, Paterson, Thut, & Gross, 2014; Gould, Rushworth, & Nobre, 2011;

99   Mok, Myers, Wallis, & Nobre, 2016; Myers, Walther, Wallis, Stokes, & Nobre, 2015; Poch,

100   Campo, & Barnes, 2014; Poch, Carretie, & Campo, 2017; Rihs, Michel, & Thut, 2007,

101   2009; Rohenkohl & Nobre, 2011; Schneider, Mertes, & Wascher, 2016; Thut, Nietzel,

102   Brandt, & Pascual-Leone, 2006; van Dijk, Schoffelen, Oostenveld, & Jensen, 2008;

103   Wallis, Stokes, Cousijn, Woolrich, & Nobre, 2015). Additionally, posterior alpha power

104   has been observed to increase with the number of items relevant after attentional

105   selection in a WM task (Jensen, 2002), also following retrospective selection (Manza,

106   Hau, & Leung, 2014; Poch et al., 2017; Poch, Valdivia, Capilla, Hinojosa, & Campo,

107   2018). Therefore, we reasoned that alpha dynamics involved in the selection of internally

108   maintained instructions should be independent of whether the task requires their

109   implementation or mere maintenance.

110   On the other hand, we hypothesized that instruction implementation relies on a specific

111   set of processes that result in the reformatting of the declarative content into action-

112   oriented code. Therefore, we expected some oscillatory features to be specifically

113   associated with proceduralization. First, the proactive reformatting of the instruction into

114   a proceduralized action-bound representation should involve the allocation of cognitive

115   control to allow the binding of stimulus and response. Ample evidence has associated

116   control-related top-down mechanisms with larger theta (3 - 7 Hz) amplitude over mid-

117   frontal scalp electrodes (Cavanagh & Frank, 2014; Cohen & Donner, 2013). Recent

118   computational models attribute to theta a central role in orchestrating long-range neural

119   communication and in binding task-relevant information (Senoussi et al., 2020; Verbeke

120   & Verguts, 2019; Verguts, 2017). At the same time, studies showed increased theta

121   power for WM manipulation (Itthipuripat, Wessel, & Aron, 2013; Onton, Delorme, &

122   Makeig, 2005). Therefore, we hypothesized stronger mid-frontal theta power during

123   preparation for instruction implementation compared to maintenance, reflecting the

124   proactive reformatting of the S-R mapping into a proceduralized action-bound

125   representation. Nevertheless, behavioral evidence suggests that only a small set of

126   mappings can be proceduralized and maintained in such a format prior to the moment of

127   their actual implementation, hinting at a limit in the number of novel instructions that can

128   be proceduralized at once (Liefooghe et al., 2012). As we expect theta power to track the

129   occurrence of such reformatting, we reasoned that theta dynamics should not differ from

130   declarative maintenance when the number of mappings to implement exceeds capacity

131   limits.

132   Finally, we reasoned that proactively recoding the instruction for execution, and not

133   merely maintaining it, should induce the preparation of the instructed motor plan

134   (Everaert, Theeuwes, Liefooghe, & De Houwer, 2014; Meiran, Pereg, Kessler, Cole, &

135   Braver, 2015a). Therefore, we looked at suppression in beta (15 – 30 Hz) and mu (8 – 12

136   Hz) frequency bands over central electrodes, oscillatory features traditionally associated

137   with motor preparation and motor imagery (Cheyne, 2013; Pineda, 2005; Rhodes, Gaetz,

138   Marsden, & Hall, 2018; Schneider, Barth, & Wascher, 2017; Tzagarakis, West, &

139   Pellizzer, 2015). We expected this modulation to be larger while preparing to implement

7

140   the instructions, thus when an action-bound procedural representation is available,

141   compared to the declarative maintenance of the mappings. Again, we predicted such

142   difference to be reduced with a higher number of instructions, due to a limit in the number

143   of action plans that can be prepared and maintained ready simultaneously.

144   To test our hypotheses, we recorded EEG activity while participants performed a task that

145   encouraged a declarative maintenance of novel S-R mappings for recognition

146   (Memorization task), and an Implementation task, intended to prompt their proactive

147   reformatting for execution. In both cases, after the presentation of four mappings at the

148   beginning of the trial, a retro-cue selected a subset of them as potential targets for the

149   subsequent recognition or execution task. We reasoned that brain activity during the Cue-

150   Target interval (CTI) would reflect the two-steps action described in a recent model of

151   information prioritization in WM (Myers, Stokes, & Nobre, 2017). According to Myers and

152   colleagues (2017), attention needs to be internally oriented towards the selected items,

153   and the prioritized representations can then be reformatted into a behavior-optimized

154   state. In the context of instruction implementation, the task-optimized representation is a

155   procedural, action-bound code of the S-R mapping. On the other hand, successful

156   maintenance is optimally achieved by means of a declarative representation of stimulus

157   and response that does not entail any action plan. Therefore, during the CTI of the two

158   tasks, we expected analogous features associated with attentional orienting, but

159   instances of reformatting to be larger in preparation for instruction implementation.

160

161   **2. Materials and Methods**

8

2.1 Participants

Thirty-nine participants took part in the experiment (M_{age} = 21.74, SD = 4.50, 33 females) and received 30 euros as compensation. Sample size was not computed a priori: we aimed for thirty-five participants, which is on the upper bound of the sample size of studies investigating similar constructs (de Vries, Van Driel, Karacaoglu, & Olivers, 2018; Schneider et al., 2017; van Ede, Chekroud, Stokes, & Nobre, 2019a). All participants had normal or corrected-to-normal vision and thirty-three reported to be right-handed. Data from two participants were discarded due to low task performance (individual mean accuracy exceeded by 2.5 standard deviations the group mean accuracy in one of the two tasks and/or accuracy in response to catch trials in one of the tasks was below 60%); data from two additional participants were discarded following visual inspection because of excessive noise in the EEG recordings, resulting in a final sample size of thirty-five participants. All participants gave their informed consent prior to the beginning of the experiment, in accordance with the Declaration of Helsinki and the protocols of Ghent University.

2.2 Materials

The same set of stimuli was used as in previous studies on instruction implementation (Formica, González-García, & Brass, 2020; González-García, Formica, Liefooghe, & Brass, 2020). It consisted of 1550 pictures, grouped in two macro categories: animate (non-human animals) and inanimate (vehicles and musical instruments) (Brady, Konkle, Alvarez, & Oliva, 2013; Brodeur, Guérard, & Bouras, 2014; Griffin, Holub, & Perona, 2007; Konkle, Brady, Alvarez, & Oliva, 2010). All images had their background removed, were centered in a 200x200 pixels square and were converted to grayscale. Stimuli

185 presentation and response collection were performed using Psychopy toolbox (Pierce,

186 2007).

2.3 Experimental design

188 Participants performed the two tasks (from now on "Implementation task" and

189 "Memorization task") in a blocked fashion during one single session, and the order of the

190 two tasks was counterbalanced between participants. The structure of the trials for the

191 two tasks was identical up to the presentation of the target (Figure 1). Each trial started

192 with a red fixation cross presented for 2000ms (± 100ms, jittered) signaling the inter-trial

193 interval and allowing participants to blink if needed, followed by a white fixation cross for

194 250ms. Next, the encoding screen containing four S-R mappings (arranged in two rows)

195 appeared for 5 seconds. Mappings consisted of a new image associated with a bimanual

196 response: "index" referred to both index fingers (keys r and i) and "middle" referred to

197 both middle fingers (keys e and o). These bilateral responses were used instead of the

198 more traditional left and right options to avoid automatic motor activations elicited by the

199 mere presentation of lateralized response words (Bundt, Bardi, Abrahamse, Brass, &

200 Notebaert, 2015). Out of the four presented mappings, two contained images of animals

201 and two images of inanimate objects. Each image-response combination was presented

202 only once during the whole duration of the experiment. The rationale of this choice was

203 to maximize WM demands and minimize the retrieval of practiced S-R mappings from

204 long-term memory (Meiran, Pereg, Kessler, Cole, & Braver, 2015b). After a 750ms delay,

205 which is considered an interval sufficiently long to discard a contribution of iconic memory

206 (Souza & Oberauer, 2016), the retro-cue appeared and remained on the screen for

207 250ms. This consisted of a square presented centrally, with one, two or four (i.e., neutral

10

208   retro-cue) colored corner(s)[1]. The number of selected mappings is the second crucial

209   factor in our design, namely Load. Participants were instructed that the retro-cue signaled

210   which mapping(s) could be probed, with 100% validity (except in the case of catch trials,

211   see below). Importantly, when the retro-cue selected two mappings, these were always

212   on the same side of the screen. The subsequent cue-target interval (CTI) had a jittered

213   duration, lasting on average 1750ms (± 100ms). This interval largely exceeds the 300 –

214   500 ms considered necessary for retro-cues to benefit performance (Souza & Oberauer,

215   2016) and sufficiently long to allow time-frequency decomposition of low frequencies

216   (Cohen, 2014b). Finally, participants were presented with the target screen, which

217   differed depending on the task. In the Implementation task, the image of one of the cued

218   mappings was presented centrally and participants were required to press the associated

219   pair of keys (both index or both middle fingers). In the Memorization task, one mapping

220   (i.e., image and associated response) was presented centrally. The image in the

221   Memorization probe belonged to one of the selected mappings (except for catch trials,

222   see below). Participants had to report whether the presented mapping matched one of

223   those selected by the retro-cue, by pressing with both fingers of one hand for "yes" or

224   both fingers of the other hand for "no". The sides for "yes" and "no" were randomly

225   assigned on a trial basis to ensure that participants could not prepare any response during

226   the CTI, therefore encouraging the mere declarative maintenance of the instruction

227   memoranda. Labels with "yes" and "no" appeared at the bottom of the target screen

228   together with the mapping. In 50% of the trials, the target screen showed the same

---

[1] The physical properties of the retro-cue could potentially produce a combination of exogenous and endogenous orienting of attention in Load 1 and 2 (i.e., one side of it is colored and thus more salient). However, we are not strongly interested in this distinction and aim at using the retro-cue as the event to locate in time the onset of different demands between tasks.

229 mapping as in the encoding ("yes" response). In the other 50% of trials, one of the

230 selected images was presented associated with a different response with respect to

231 encoding ("no" response). Crucially, despite the similarities in trial structure, the

232 Memorization task relied on the declarative maintenance of the mappings as no response

233 could be prepared, whereas the Implementation task encouraged a proactive preparation

234 of the selected mappings for the execution of the required action plan. Both tasks included

235 catch trials (~25% for each task), in which the target screen displayed a different image

236 than the four displayed in the encoding screen. In this case, participants were required to

237 press the spacebar. This was done to discourage participants to adopt specific strategies,

238 such as memorizing only the mappings associated with one response option. Since we

239 were interested in the brain activity before the onset of the target, EEG recordings from

240 catch trials were analyzed together with regular trials. For each task, participants

241 completed 5 experimental blocks, for a total of 180 trials (60 per load, Figure 1).

242 Each of the two tasks was preceded by a practice session. This consisted of mini-blocks

243 of 12 trials, including all possible load conditions (i.e. number of mappings selected by

244 the retro-cue) and at least one catch trial. The only difference with the main task was the

245 presence of feedback at the end of each trial, signaling the accuracy of the response or

246 encouraging participants to respond faster in case no response was registered within the

247 maximum response time of 3 seconds. Performance was assessed at the end of each

248 mini-block: if accuracy was above 80%, practice was concluded, otherwise a new mini-

249 block started, up to a maximum of 3 blocks. S-R mappings used during the practice were

250 never presented again during the main task. The total duration of the experiment,

251 including cap preparation, practice, main tasks and breaks was approximately 150
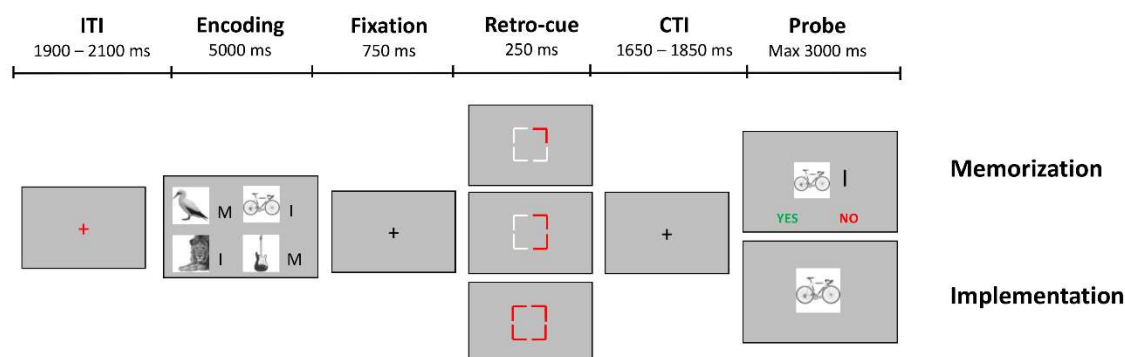
252 minutes.

253

254 **Figure1: Behavioral paradigm.** Participants had to first encode four S-R mappings, for subsequent

255 recognition (Memorization task) or for a choice-reaction task (Implementation task). During the retention

256 interval, a Retro-Cue selected one, two or all four mappings as relevant for the upcoming probe. Participants

257 performed the two tasks separately in a block design.

258

259 *2.4 EEG Recordings and pre-processing*

260 Electrophysiological data were recorded using a BioSemi ActiveTwo system (BioSemi,

261 Amsterdam, Netherlands) with 64 Ag–AgCl electrodes arranged in the standard

262 international 10–20 electrode mapping (Klem, Lüders, Jasper, & Elger, 1999), with a

263 posterior CMS-DRL electrode pair. Two reference electrodes were positioned at the left

264 and right mastoids. Eye movements were registered with a pair of electrodes above and

265 below the left eye and two additional electrodes at the outer canthi of both eyes. EEG

266 signals were recorded at a 1024 Hz sampling rate.

267 EEG data were preprocessed using the Fieldtrip toolbox (Oostenveld, Fries, Maris, &

268 Schoffelen, 2010), running in MATLAB (MATLAB R2017b, The MathWorks, Inc., Natick,

269 Massachusetts, United States). First, the data were downsampled to 512 Hz and re-

270 referenced to the average of the mastoids. Then, a $0.5 - 45$ Hz band-pass FIR filter was

271 applied to the data, together with a Notch filter at 50 Hz and its harmonics. Data were

272 epoched relative to the onset of the retro-cue (from -1000 to 2500 ms) and demeaned to

273 the average of the whole epoch, to improve independent component analysis (ICA)

274 (Groppe, Makeig, & Kutas, 2009). Only trials in which the participant performed the

275 correct response were retained for subsequent analyses. Trials exhibiting movement

276 artifacts or excessive noise were removed following visual inspection of the data. Next,

277 eye movements artifacts were removed by means of ICA, using the EEGLAB (Delorme

278 & Makeig, 2004) runica algorithm as implemented in Fieldtrip. Components to discard

279 were selected based on their topography, the correlation between their time course and

280 the horizontal and vertical electrooculography, and their power spectrum. For most

281 participants, two components were removed (capturing blinks and horizontal eye

282 movements, respectively); in six participants blinks were reflected in two components,

283 leading to the removal of three IC, and in two participants only one component was

284 removed. Finally, data were visually inspected again to ensure successful cleaning and

285 one (N = 6), two (N = 2) or three (N = 1) excluded channels were interpolated by means

286 of spherical spline interpolation (Perrin, Pernier, Bertrand, & Echallier, 1989). This

287 cleaning procedure resulted in an average of 151.09 trials for the Implementation task

288 (*SD* = 12.29, 83.94%) and 143.06 trials for the Memorization task (*SD* = 14.07, 79.48%).

289 For each load condition, an average of 81.7% of trials were retained (Implementation,

14

290   Load 1: 52.14 (*SD* = 3.64) trials, Load 2: 50.26 (*SD* = 5.19) trials, Load 4: 48.68 trials (*SD*

291   = 5.74); Memorization, Load 1: 49.88 trials (*SD* = 4.84), Load 2: 47.86 trials (*SD* = 5.86),

292   Load 4: 45.31 trials (*SD* = 5.94).

293   *2.5 Spectral Analysis*

294   For each Task x Load condition (Memorization-Load 1, Memorization-Load 2,

295   Memorization-Load 4 and Implementation-Load 1, Implementation-Load 2,

296   Implementation-Load 4), time-frequency analysis was performed separately using

297   complex Morlet wavelet convolution, to estimate spectral power from 1 to 45 Hz in steps

298   of 1 Hz. The number of cycles in the wavelet was frequency-specific, ranging from 2 at 1

299   Hz and linearly spaced up to 7 cycles at 45 Hz, to achieve a good trade-off between

300   temporal and frequency precision (Cohen, 2014a). This analysis resulted in one time-

301   frequency spectrogram for each channel, condition and participant. Condition-specific

302   decibel normalization was then applied, using the time window between -500 and -200ms

303   before the onset of the retro-cue as baseline. To avoid data contamination due to the

304   smearing in time of the processing of the target, all statistical analyses are performed on

305   the time window from 0 to 1800ms with respect to retro-cue onset, therefore leaving

306   100ms gap between the end of our analyses window and the earliest jittered target onset.

307   *2.6 Statistical Analyses*

308   Reaction times (RTs), error rates (ER) and averaged alpha power (see below) were

309   separately entered in 2 (Task: Memorization vs Implementation) x 3 (Load: 1, 2, 4)

310   repeated measure ANOVAs, performed in JASP (Jasp Team, 2019).

15

311   To evaluate the statistical significance of differences between EEG time-courses or time-

312   frequency spectra, we adopted a cluster-based permutation approach (Maris &

313   Oostenveld, 2007), which is appropriate to assess the reliability of neural patterns over

314   neighboring data points. Moreover, this approach is robust against the multiple-

315   comparison problem, as the significance of clusters found in the observed group-level

316   data is estimated against a distribution of clusters obtained by randomly permuting the

317   assignement of participants to each group. First, depending on the number of conditions

318   to be compared, we performed either a two-sided t-test (two conditions) or an F-test (three

319   conditions), at an α level of 0.05, between all data points of the observed conditions.

320   Then, we considered as cluster a group of adjacent data points with same sign

321   significance and as cluster-size the sum of all t- or F-values in the cluster. Next, we used

322   5,000 permutations of participant-level data to estimate a distribution of cluster sizes

323   under the null hypothesis that there were no differences between conditions. The *P*-value

324   for each cluster in the observed group-level data corresponds to the proportion of

325   permutations in which the largest cluster size was larger than the size of the considered

326   observed cluster. Again, we used a significance alpha level of 0.05, therefore only

327   observed clusters whose size was larger than the size of the largest cluster in at least

328   95% of permutations are reported. This approach provides a statistically sound procedure

329   to compare two conditions and establish the existence of a difference between them,

330   reliably accounting for multiple comparisons. However, because clusters found through

331   this procedure reflect the result of the second level inference between the observed and

332   the null permuted distributions, no strong conclusions can be drawn with respect to their

333 boundaries, such as the exact latency or frequency range of the effect (Sassenhagen &

334 Draschkow, 2019).

2.7 Contralateral alpha suppression

336 Consistent findings reported alpha desynchronization over posterior regions contralateral

337 to the attended spatial location, indicating top-down anticipatory mechanisms of

338 attentional orienting in the perceptual or internal space (Bonnefond & Jensen, 2012;

339 Capilla et al., 2014; Gould et al., 2011; Jensen & Mazaheri, 2010; Mok et al., 2016; Myers

340 et al., 2015; Rihs et al., 2007, 2009; Rohenkohl & Nobre, 2011; Sauseng et al., 2005;

341 Thut et al., 2006; van Dijk et al., 2008; Wallis et al., 2015).

342 To estimate the suppression of alpha oscillations contralateral to the cued hemifield, we

343 averaged the time-frequency spectra corresponding to Load 1 and Load 2, separately for

344 the two tasks. Trials with neutral retro-cues (Load 4) were excluded from this analysis

345 because they did not induce attentional orienting towards one of the two visual hemifields.

346 Based on previous literature, two pairs of electrodes were selected in right (P8, PO8) and

347 left (P7, PO7) posterior parietal regions (de Vries, van Driel, & Olivers, 2019a; Gould et

348 al., 2011; Schneider et al., 2017; van Ede, Chekroud, Stokes, & Nobre, 2019b). Power

349 spectra were extracted from these electrode pairs, averaged in the alpha frequency range

350 (8 – 14 Hz), and collapsed between retro-cues pointing to the left and right hemifield, in

351 order to extract one power time series for the contralateral hemisphere and one for the

352 ipsilateral hemisphere. The two time series were compared by means of cluster-based

353 permutation testing, separately for the two tasks (see Statistics section). Additionally, the

354 cluster-based permutation approach was also used to compare the contralateral alpha

355 suppression between the two tasks. Namely, for each task the ipsilateral power time

356 series was subtracted to the contralateral one, separately for each participant, and the

357 resulting difference waves were compared. This analysis was performed to test whether

358 the deployment of alpha oscillations to orient attention towards relevant mental

359 representations differed between tasks.

360   *2.8 Load-dependent alpha increase*

361 Posterior alpha power has been observed to increase with the number of items relevant

362 after attentional selection in a WM task (Fukuda, Mance, & Vogel, 2015; Jensen, 2002),

363 also following retrospective selection (Manza et al., 2014; Poch et al., 2017, 2018).

364 Observing such modulation in our data would be evidence in favor of an effective selection

365 of the relevant mappings. To investigate the increase in alpha power relative to the

366 number of retained items, we extracted the average power for the frequencies ranging

367 from 8 to 14 Hz, separately for each condition and task, from the electrode pair Pz and

368 POz (Jensen, 2002), across the whole time window from 0 to 1800ms with respect to the

369 onset of the retro-cue. This operation led to one averaged alpha power value for each

370 Task-Load combination per participant, that were entered in a 2 (Task) x 3 (Load)

371 repeated measure ANOVA.

372   *2.9 Mid-frontal theta in Implementation*

373 The two tasks differ to the extent they require the reformatting of the encoded information

374 in an action-oriented code. We hypothesized such transformation to rely on a top-down

375 mechanism supported by low frequency oscillations. To test our predictions, time-

376 frequency spectra were extracted from the CTI (0 – 1800 ms) in the frequency range 3 –

377 7 Hz, averaged from channels Fz and AFz. The choice of these two channels was guided

378 by both their widespread use in the literature concerning midfrontal theta (Berger et al.,

379 2019; Cooper et al., 2019; Onton et al., 2005; Popov et al., 2018; Senoussi et al., 2020)

380 and a condition-independent channel selection procedure. Namely, we fitted the power

381 spectra from all channels, computed across all trials, regardless of the Load condition

382 and the Task, with the FOOOF toolbox (Haller et al., 2018). This method allows to

383 decompose different components of the power spectrum (i.e., the aperiodic (1/f pattern)

384 and periodic components) and thus to better capture the oscillatory profile of

385 electrophysiological data. This analysis confirmed that, across conditions, channels Fz

386 and AFz exhibited the largest peaks in the power spectra between 3 and 7 Hz (see

387 Supplementary materials for details).

388 We tested the main effect of Task by comparing the time-frequency spectra of

389 Implementation and Memorization (averaged across levels of Loads) by means of cluster-

390 based permutation test. Similarly, we tested the main effect of Load by contrasting the

391 spectra for each level of Load, averaged across Task condition. We then tested for a

392 significant effect of the interaction between our two factors by running a cluster-based

393 permutation test on the three time-frequency spectra resulting from pairwise subtraction

394 of the two tasks for each Load level (i.e., Implementation 1 minus Memorization 1,

395 Implementation 2 minus Memorization 2 and Implementation 4 minus Memorization 4).

396 *2.10 Motor-related mu and beta suppression in Implementation*

397 Analogously, we hypothesized that action-oriented procedural representations should

398 entail a motor plan, reflected in stronger signatures of proactive motor preparation. We

399 expected differences in two frequency bands associated with motor preparation, namely

400 mu (8 -12 Hz) and beta (15 – 30 Hz) (Cheyne, 2013; Pineda, 2005). To test for this, we

19

401 extracted time-frequency spectra averaged across electrodes C3 and C4 from the CTI (0

402 – 1800 ms). Next, we again used a cluster-based permutation approach outlined for mid-

403 frontal theta, to look for significant clusters of different activity between tasks, loads, and

404 their interaction. We selected electrodes C3 and C4 because we expected the effect to

405 be maximal over motor and pre-motor cortices[2] (Marchesotti, Bassolino, Serino, Bleuler,

406 & Blanke, 2016; McFarland, Miner, Vaughan, & Wolpaw, 2000). Moreover, we averaged

407 across the two of them because the goal of this comparison was to investigate pre-

408 movement preparatory oscillatory activity, rather than the effector-specific M1 activation

409 (Neuper & Pfurtscheller, 2001; Pfurtscheller, Brunner, Schlögl, & Lopes da Silva, 2006;

410 Pfurtscheller & Neuper, 1997). In our study, responses were bimanual in the

411 Implementation task and lateralized in the Memorization task. However, we reasoned that

412 our test is independent of such difference, as before target onset responses from both

413 hands had to be prepared in the two tasks.

414

415 **3. Results**

416 *3.1 Behavioral results*

417 Concerning behavioral performance, we expected valid retro-cues to have a beneficial

418 effect on reaction times and error rates in both tasks (Souza & Oberauer, 2016). Repeated

---

[2] Electrodes selection for analyses in the mu and beta frequency ranges was based on the literature and on the clearer assumptions on the brain areas causing the expected oscillations (i.e., pre-SMA and M1). Moreover, we chose to not rely on an independent electrode selection as we did for theta because the FOOOF toolbox results in higher frequencies are more susceptible to muscular artifacts and therefore less accurate.

419   measures ANOVA on RTs confirmed a significant main effect of Load[3] ($F_{1.44,\ 49.06}$ =

420   104.65, $p < 0.001$, $\eta^2_p = 0.76$): RTs increased with the number of mappings selected by

421   the retro-cue (Load 1: M = 978ms, SD = 196, Load 2: M = 1168ms, SD = 150, Load 4: M

422   = 1266ms, SD = 142). The main effect of Task was also significant ($F_{1,\ 34}$ = 237.20, $p <$

423   0.001, $\eta^2_p = 0.87$), with slower RTs in Memorization (M = 1355ms, SD = 185) than

424   Implementation (M = 907ms, SD = 160). The interaction between the two factors also

425   resulted to be significant ($F_{1.32,\ 44.88}$ = 4.42, p = 0.031, $\eta^2_p = 0.11$). More specifically, the

426   effect of Load was larger in the Implementation task ($F_{1.44,\ 49.06}$ = 93.20, $p < 0.001$)

427   compared to the Memorization task ($F_{1.44,\ 49.06}$ = 45.50, $p < 0.001$) (Figure 2a).

428   Error rates showed a significant main effect of Task ($F_{1,\ 34}$ = 11.08, p = 0.002, $\eta^2_p = 0.25$)

429   and of Load ($F_{1.67,\ 57.91}$ = 25.65, $p < 0.001$, $\eta^2_p = 0.43$). Participants were significantly

430   more accurate in the Implementation task (M = 0.14, SD = 0.09) compared to the

431   Memorization task (M = 0.19, SD = 0.10), and were more accurate when less items were

432   selected by the retro-cue (Load 1: M = 0.12, SD = 0.07, Load 2: M = 0.17, SD = 0.10,

433   Load 4: M = 0.20, SD = 0.12). The interaction between the two factors was not significant

434   (p = 0.266) (Figure 2b).

435   Regarding catch trials, participants could successfully detect a new image in both the

436   Memorization task (error rate in catch trials: M = 0.13, SD = 0.08) and the Implementation

437   task (M = 0.09, SD = 0.07). Nevertheless, they were significantly less accurate (t_{34} = 3.16,

438   p = 0.003, d = 0.53) in the Memorization task.

---

[3] Mauchly's test revealed that the assumption of sphericity is violated ($p < 0.05$). Greenhouse-Geisser correction is applied here and in all results where the sphericity assumption is violated.

439   Such differences in performance between Implementation and Memorization are not

440   surprising and can be at least partially attributed to the task-specific processes taking

441   place after the occurrence of the target (Formica et al., 2020; Muhle-Karbe et al., 2017).

442   Specifically, the Memorization task requires the comparison of the presented mapping to

443   the encoded ones, the identification of the response side, and the execution of the

444   intended response. On the contrary, the Implementation task only involves the

445   identification of the target stimulus and the execution of the associated motor response.
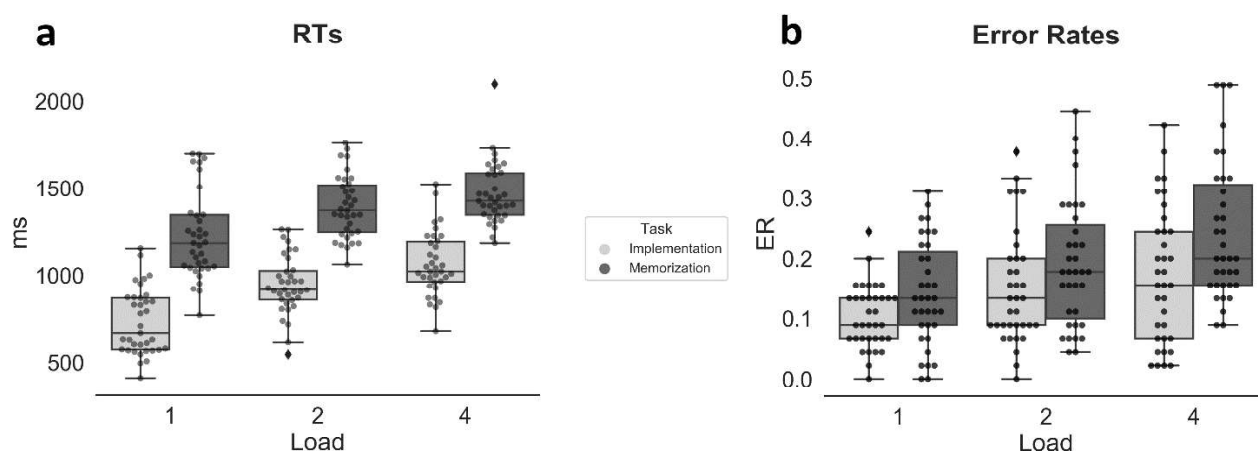

446

447   **Figure 2: Behavioral results**. **a**) Reaction times (ms). **b**) Error rates. Both measures confirmed a benefit

448   in performance (i.e., faster RTs and less errors) when the Retro-Cue selected less mappings. In each

449   boxplot, the thick line inside box plots depicts the second quartile (median) of the distribution (n = 35). The

450   bounds of the boxes depict the first and third quartiles of the distribution. Whiskers denote the 1.5

451   interquartile range of the lower and upper quartile. Dots represent individual subjects' scores.

452

453   *3.2 EEG Results*

454   *3.2.1 Contralateral alpha power decrease*

455   As hypothesized, we observed a stronger reduction in alpha power in contralateral

456   compared to ipsilateral electrodes across loads 1 and 2 both in Implementation ($P =$

457   0.013, cluster-corrected) and Memorization ($P = 0.003$, cluster-corrected) tasks (see

458   Supplementary material for the same analysis performed separately for the two load

459   conditions). The significant clusters spanned the time window around 600 – 800ms.

460   Notably, we did not find any difference between the two tasks (no cluster survived multiple

461   comparison correction, even at a cluster threshold of $P = 0.1$), supporting our hypothesis

462   that the mechanisms allowing for attentional orienting are engaged to a similar extent in

463   the two tasks (Figure 3a). To qualitatively confirm our electrodes selection and the

464   location of the significant effect, contralateral minus ipsilateral half-topographies are

465   reported separately for each task (Figure 3b).

466

467   *3.2.2 Load-dependent alpha increase*

468   We predicted alpha power to also track the number of items selected by the retro-cue to

469   be relevant for the ongoing task. The repeated measures ANOVA on the averaged alpha

470   power over Pz – POz in the whole CTI (0 – 1800ms) revealed a significant main effect of

471   Load ($F_{2, 68} = 24.81$, $p < 0.001$, $\eta^2_p = 0.42$) (Figure 3c). Specifically, alpha power values

472   increased with the number of retained items (Load 1 vs Load 2: $t = -3.24$, $p = 0.006$

473   Bonferroni-corrected; Load 2 vs Load 4: $t = -3.38$, $p < 0.001$ Bonferroni-corrected), both

474   in Implementation (Load 1: $M = 0.83$, $SD = 1.83$, Load 2: $M = 1.12$, $SD = 1.83$, Load 4: M

475    $= 1.42$, $SD = 1.92$) and Memorization (Load 1: $M = 0.77$, $SD = 1.78$, Load 2: $M = 1.22$,

476    $SD = 1.87$, Load 4: $M = 1.79$, $SD = 1.90$). Crucially, neither the effects of Task nor the

477   interaction Task x Load were significant (ps > 0.1). Scalp topographies of alpha power

478   across the entire CTI are reported separately for each Task and Load condition (Figure
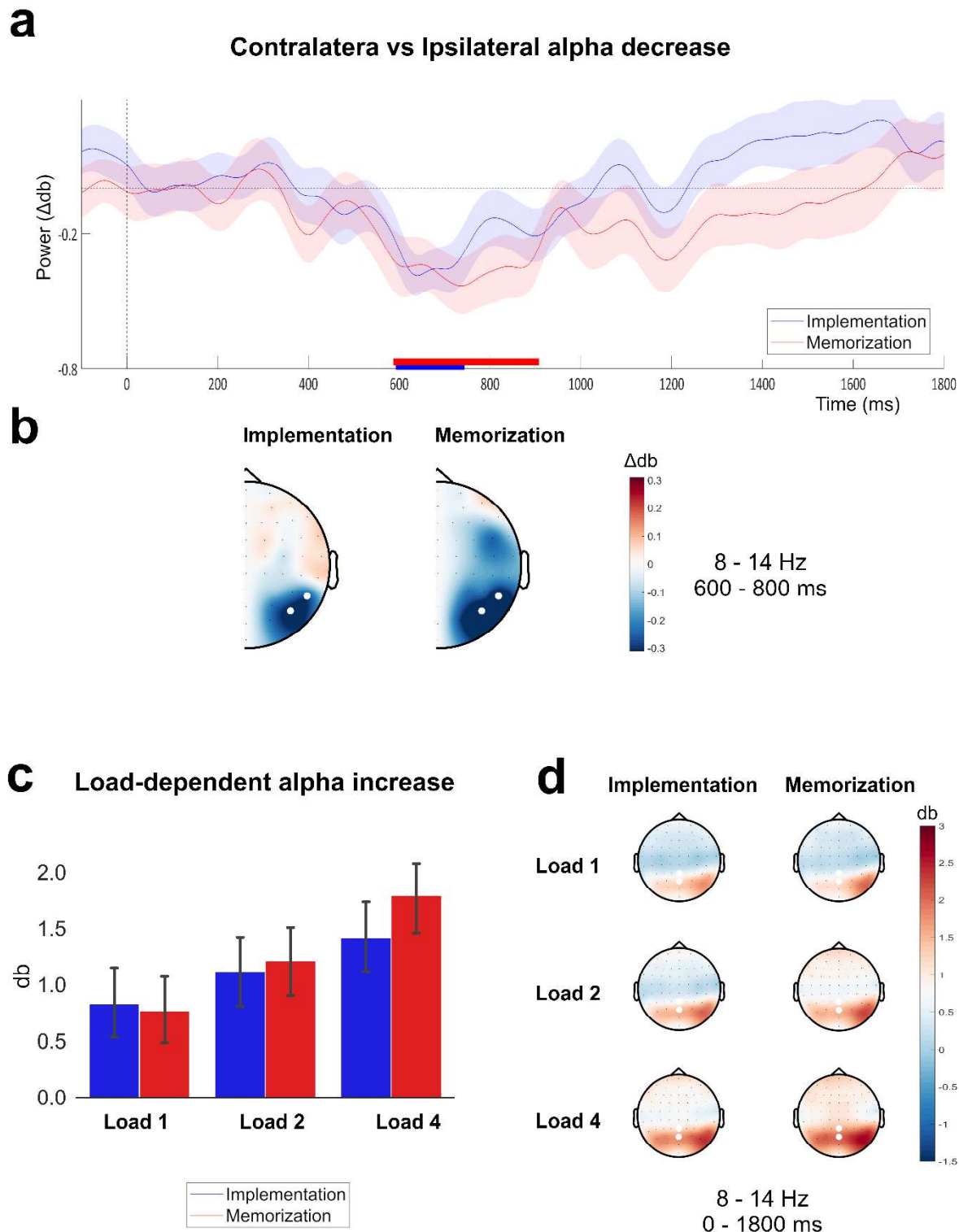
479   3d).

Figure 3: Alpha power dynamics. **a**) Time courses of the difference waves (contralateral minus ipsilateral time course) of alpha power activity between contralateral and ipsilateral electrode clusters (PO8 - P8 and

483   PO7 - P7). Both difference waves show a significant deflection from 600 to 800ms after the onset of the

484   retro-cue. Horizontal lines above the x-axis indicate significant temporal clusters (blue: Implementation, red:

485   Memorization), obtained with cluster-based permutation testing). Shading represents the s.e.m., calculated

486   across participants (n = 35). **b**) Half topographies showing differences in alpha power for contralateral minus

487   ipsilateral electrodes collapsed across hemispheres. White dots indicate the a-priori selected electrodes

488   used in the cluster-based permutation analysis. **c**) Alpha power values averaged in the time window 0 –

489   1800 ms after Retro-Cue onset from electrodes Pz and POz. Error bars represents the s.e.m. calculated

490   across participants (n = 35). **d**) Topographies of each Task x Load condition. White dots indicate the a-

491   priori selected electrodes (Pz and POz) from which activity was extracted for the ANOVA.

492

3.2.3 Mid-frontal theta in Implementation

494   We expected to find stronger theta power over mid-frontal electrodes in the

495   Implementation task compared to the Memorization task. Supporting this prediction, we

496   found a significant cluster (P = 0.04, corrected for multiple comparisons) when comparing

497   the power estimates of the two tasks in the frequency range 3 – 7 Hz from electrodes Fz

498   and AFz (Figure 4). On the contrary, the test aimed at detecting a main effect of Load

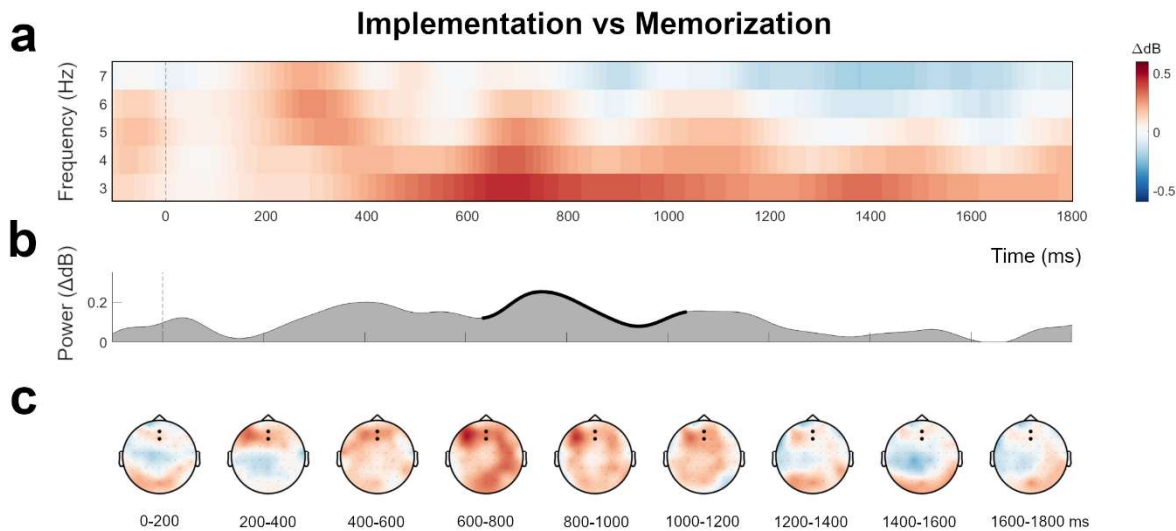499   approached but did not reach significance (P = 0.09).

Figure 4: Theta dynamics in Implementation compared to Memorization. a) Time-frequency power spectrum extracted from the electrodes Fz and AFz. **b**) Averaged power time course (3 – 7 Hz) from the electrode Fz and AFz. Thicker outline indicates timepoints belonging to the significant cluster. **c)** Each topography represents the averaged activity in the frequency range 3 – 7 Hz, in 200 ms time windows within the CTI (0 – 1800 ms). Black dots indicate the electrodes used for the statistical analysis.

Moreover, our corollary hypothesis concerning theta dynamics predicted such effect to be modulated by the number of mappings to be implemented or memorized. Specifically, we expected that in Load 4 Implementation and Memorization would not differ, in line with behavioral findings showing that 4 novel instructions cannot be proceduralized at once and would therefore be maintained in a declarative format in both conditions (Liefooghe et al., 2012). However, the effect of the interaction resulted to be not significant (P = 0.53). Despite the lack of a significant interaction, and thus the impossibility to draw any strong conclusion from post-hoc tests, we explored the effect of Task across different Load levels by means of pairwise comparisons. We observed a significant cluster only in the contrast

516 Implementation 2 vs Memorization 2 (P = 0.02), whereas no cluster was observed for

517 Load 4, and no cluster survived correction in Load 1 (P = 0.23).

518 One potential confound when investigating activity in low frequency bands is that this

519 might be reflecting sustained ERPs. To rule out this possibility we compared across tasks

520 the Contingent Negative Variation (CNV), a slow negative potential over centro-frontal

521 electrodes during preparation for an upcoming target (Walter, Cooper, Aldridge,

522 McCallum, & Winter, 1964). The CNV did not show a differential pattern between

523 Implementation and Memorization (see Supplementary material), suggesting that our

524 frontal activity is better described by low frequency oscillations, rather than a sustained

525 ERP. Furthermore, at the lowest estimated frequency of 2 Hz, the wavelet was two-cycles

526 long, i.e. spanning a 1s interval, which is considered to be selective to true oscillations

527 and able to disentangle them from non-oscillatory signal (Cohen, 2014a). Finally,

528 interpreting this frontal activity as the correlate of target expectancy would not account for

529 the effect specific to Load 2 observed in time-frequency analyses.

530 *3.2.4 Motor-related mu and beta suppression in Implementation*

531 We hypothesized that proceduralization would induce increased recruitment of motor and

532 premotor regions, in preparation for the instructed upcoming movement, compared to

533 Memorization. Specifically, we predicted a suppression of oscillations in the mu (8 – 12

534 Hz) and beta (15 – 30 Hz) frequency ranges, which have been shown to reflect motor

535 cortex activity (Cheyne, 2013; Pineda, 2005; Rhodes et al., 2018; Schneider et al., 2017;

536 Tzagarakis et al., 2015). To test for this hypothesis, we again used cluster-based

537 permutations and we tested the effects of Task, Load, and their interaction, separately for

538 each frequency range of interest (i.e. mu and beta).

28

539   In line with our prediction, we found significant clusters when contrasting the two Tasks

540   both in the mu (P = 0.01) and beta (P = 0.03) frequency ranges. This finding supports the

541   idea that proceduralization involves a recruitment of motor areas for the activation of the

542   instructed motor plan (Figure 5).
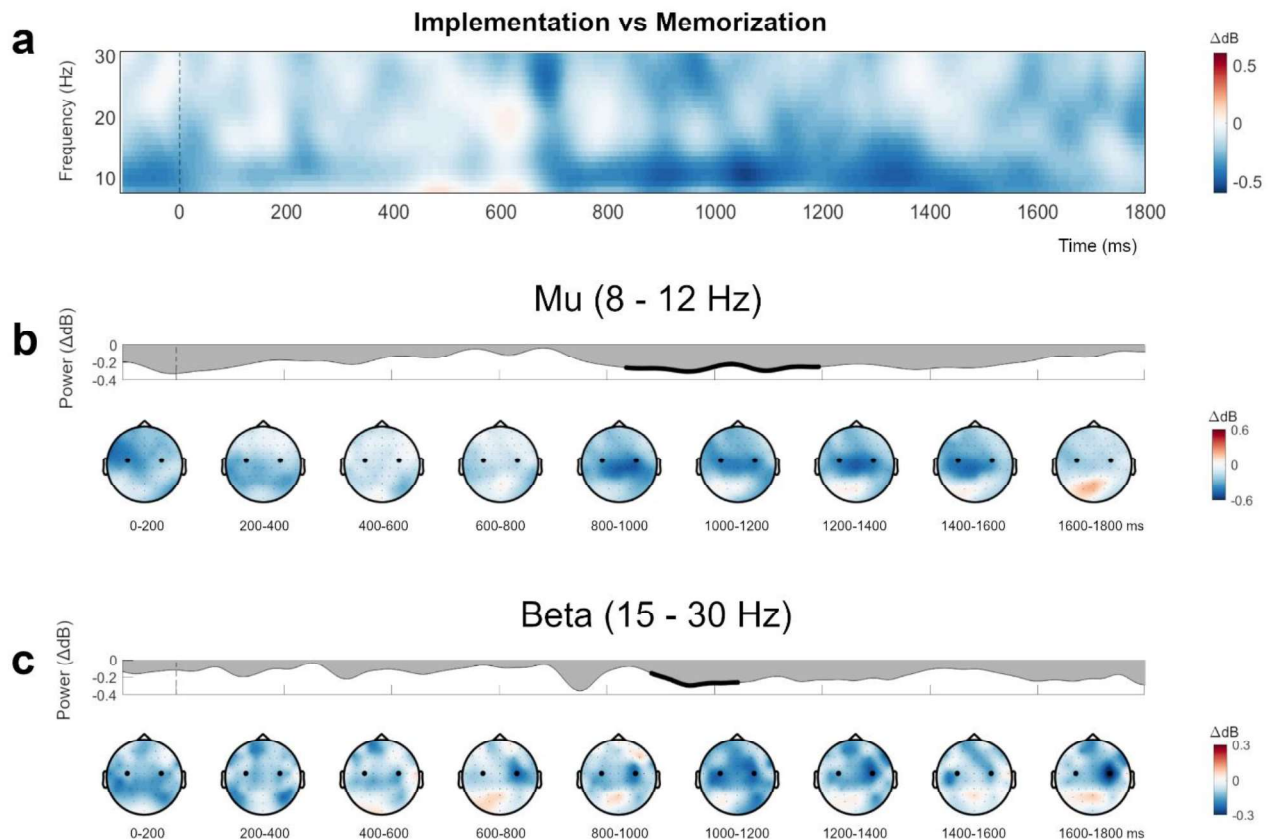

543

544   **Figure 5: Mu and Beta dynamics in Implementation compared to Memorization. a)** Time-frequency

545   power spectrum from electrodes C3 and C4. **b)** Averaged power time course in the Mu (8 − 12 Hz)

546   frequency range from electrodes C3 and C4: thicker outline indicates timepoints belonging to the significant

547   cluster. Topographies in 200 ms time windows: black dots indicate the electrodes used for statistical

548   analyses. **c)** Averaged power time course in the Beta (15 − 30 Hz) frequency range from electrodes C3 and

549   C4: thicker outline indicates timepoints belonging to the significant cluster. Topographies in 200 ms time

550   windows: black dots indicate the electrodes used for statistical analyses.

551   Similarly, the effect of Load resulted to be significant in both mu (P < 0.001) and beta (P

552   < 0.001) range, suggesting that these motor-related oscillatory features are also sensitive

553   to the number of items being handled.

554   As for theta, our secondary hypothesis was that the differences in mu and beta dynamics

555   between tasks would be modulated by the number of mappings. This hypothesis would

556   be in line with a capacity limit in the amount of instructions that can be proceduralized at

557   once, and thus converted in an action plan. However, in neither of the two frequency

558   bands the cluster-based permutations tests revealed significant clusters for an effect of

559   such interaction (mu: P = 0.14, beta: P = 0.57). As exploratory follow-up analyses we

560   performed pairwise comparisons separately for each Load level (i.e., Implementation 1

561   vs Memorization 1, Implementation 2 vs Memorization 2, Implementation 4 vs

562   Memorization 4). Although interpretations of these results have to be cautious and do not

563   allow to draw any strong statistical conclusion, it is interesting to observe that again only

564   in Load 2 the two tasks showed clusters of different activity (beta: P1 < 0.001, P2 = 0.02,

565   P3 = 0. 21, mu: P1 = 0.003, P2 = 0.006, P3 = 0.042). On the contrary, comparisons in

566   Load 1 (beta: P = 0.19, mu: no cluster) and Load 4 (beta: P = 0.35, mu: P = 0.13) yielded

567   no significant clusters.

568

569   **4. Discussion**

570   In the present study, we investigated the spectral and temporal dynamics underlying

571   novel instruction implementation. In line with our predictions and the framework proposed

572   by Myers and colleagues (2017), we observed an analogous unfolding of early attentional

573 mechanisms across tasks, reflected in similar patterns of alpha power dynamics.

574 Crucially, Implementation and Memorization also showed differences in frontal theta, and

575 central mu and beta oscillations, suggesting that Implementation-specific processes go

576 beyond the attentional prioritization of the relevant items. These mechanisms are likely

577 involved in the reformatting of the selected S-R mappings into a behavior-optimized,

578 action-bound process requiring the exertion of cognitive control and resulting in the

579 preparation of the instructed motor plan (van Ede, 2020).

580 An underlying assumption of our study is that the intention to implement the instructed

581 mappings is a crucial necessary factor to trigger the reformatting from declarative to

582 procedural state (Liefooghe et al., 2012). This exclusive role of the intention to implement

583 has been questioned by some recent behavioral evidence, suggesting an automatic

584 reformatting of the instruction independent of task demands (Liefooghe & De Houwer,

585 2017). This might be due to the response set used in the specific task, or to other

586 idiosyncratic factors. Despite these inconsistencies in the behavioral measures, the

587 dissociation between Implementation and Memorization is well established at the neural

588 level (Demanet et al., 2016; González-García et al., 2019; Muhle-Karbe et al., 2017).

589 Here, we show such differences are reflected in oscillatory mechanisms.

590 *4.1 Alpha-mediated attentional orienting is analogous in Implementation and*

591 *Memorization*

592 Activity in the alpha frequency band has been consistently associated with attentional

593 processing (van Ede, 2017). In particular, posterior alpha power decreases over posterior

594 electrodes contralateral to the attended hemifield, both in perceptual and in WM tasks

595 (Jensen & Mazaheri, 2010; Poch et al., 2017; Sauseng et al., 2005). In our experiment,

596 participants were encouraged to focus on the selected items and discard the unselected

597 ones. Coherently, in both tasks we found after the retro-cue a significant suppression of

598 alpha oscillations contralateral to the attended hemifield. The most influential model

599 proposed to account for this phenomenon is referred to as *Gating by Inhibition* (Jensen &

600 Mazaheri, 2010). According to this framework, top-down alpha modulation of sensory

601 cortices allows for the inhibition of irrelevant inputs, contributing to the creation of a

602 functional network optimized to perform the task (Mazaheri et al., 2014; Van Diepen,

603 Foxe, & Mazaheri, 2019). Our clusters of alpha lateralization extended around 600 –

604 800ms after retro-cue. This dynamic is consistent with previous findings on lateralized

605 retrospective orienting of internal attention, showing modulations within 500 and 1000ms

606 (Mok et al., 2016; Poch et al., 2017, 2018; Wallis et al., 2015; Wolff, Ding, Myers, &

607 Stokes, 2015; Wolff, Jochim, Akyürek, & Stokes, 2017). The occurrence of the selection

608 process is further supported by load-dependent centro-posterior alpha power modulation.

609 The amplitude of alpha power has been observed to be sensitive to the number of items

610 retained during a WM task (Fukuda et al., 2015; Jensen, 2002). In both our tasks, alpha

611 increased with load. Crucially, we observed no task-dependent differences in the

612 dynamics of alpha oscillations, suggesting that the information provided by the retro-cue

613 is used to analogously orient attention and select the items that are likely to be probed,

614 independently of task demands.

615   *4.2 Low frequencies oscillations for S-R binding in Implementation*

616 We predicted low frequency oscillations over frontal sensors to be associated with the

617 proactive reformatting of the S-R mapping(s) into an action-oriented code. The crucial

618 contribution of the PFC in quickly converting symbolic instructions into task-sets for

619 prospective action has been widely established in several fMRI studies (Brass, Wenke,

620 Spengler, & Waszak, 2009; Cole, Bagic, Kass, & Schneider, 2010; Dumontheil,

621 Thompson, & Duncan, 2011; González-García et al., 2017; Hartstra et al., 2011;

622 Palenciano, González-García, Arco, & Ruz, 2019; Ruge & Wolfensteller, 2010). In

623 particular, declarative maintenance and implementation of novel mappings can be

624 dissociated using univariate and multivariate analyses in prefrontal regions, such as the

625 inferior frontal junction (IFJ) and the inferior frontal sulcus (IFS) (Bourguignon et al., 2018;

626 Demanet et al., 2016; Hartstra et al., 2011; Muhle-Karbe et al., 2017). Activation of these

627 areas has been interpreted as reflecting the creation and the activation of procedural

628 condition-action rules from the instructed mappings, a process that is thought to involve

629 the manipulation of the available information and the exertion of cognitive control (Brass

630 et al., 2017). Analogously, the need for top-down control over complex goal-directed

631 cognitive operations is traditionally linked with oscillations in the theta frequency range

632 over prefrontal cortices (Cavanagh & Frank, 2014; Cooper et al., 2019). Moreover, recent

633 influential models of large-scale brain interactions attribute to theta the crucial role of

634 orchestrating information exchange between distant areas by synchronizing their firing

635 pattern (Fries, 2005, 2015; Lisman & Jensen, 2013; McLelland & VanRullen, 2016;

636 Verguts, 2017). We hypothesized the Implementation task in our experiment to require a

637 more extensive allocation of cognitive control, given the need to manipulate the

638 declarative representations of the selected S-R mappings into their procedural

639 counterparts, leading to increased power in low frequencies over frontal sensors.

640 Supporting this prediction, our Implementation and Memorization tasks differed in the

641   extent to which they engaged oscillations in the theta frequency range over prefrontal

642   regions.

643   Previous studies show mixed findings with respect to the role of midfrontal theta power in

644   dissociating maintenance and manipulation of WM items. Berger and colleagues (2019)

645   reported no differences in theta power between retention and mental spatial mirroring

646   (i.e., manipulation) of a grid of colored dots. On the contrary, the study by Itthipuripat and

647   colleagues (2013) used a sequence updating paradigm and revealed increased theta for

648   both contrasts Manipulation vs Maintenance and Manipulation (correct trials) vs

649   Manipulation (incorrect trials). Interestingly, they found low theta (2 − 4 Hz) to be sensitive

650   to manipulation demands, whereas high theta (5 − 7 Hz) increased in both contrasts

651   (Itthipuripat et al., 2013). Although the exact boundaries of our significant cluster cannot

652   be strongly interpreted due to the nature of the statistical approach we adopted (see

653   statistical Methods section), the effect of Task we find in our study appears to be

654   predominant in the lower frequencies. One possibility is that different frequencies within

655   the theta band serve different cognitive functions. This view has recently been gaining

656   support. Evidence in favor of a more fine-grained characterization of theta oscillations

657   include variations in theta peak frequency depending on task demands and difficulty

658   (Senoussi et al., 2020), and differences in the functional significance of high (posterior)

659   and low (anterior) hippocampal theta (Goyal et al., 2020).

660   A functional role has been attributed to theta oscillations in the prioritization of relevant

661   information in visual WM. Oscillations in the delta/low theta (2 − 6 Hz) range have been

662   observed during switches of internal attention from one search template to another for

663   prospective use (de Vries et al., 2018; de Vries, van Driel, & Olivers, 2019b; Senoussi et

664   al., 2019). Such involvement has also been causally tested by applying rhythmic (5 Hz)

665   and arrhythmic transcranial magnetic stimulation to the lateral PFC during a change

666   detection task with retro-cues (Riddle et al., 2020). Rhythmic stimulation caused an

667   entrainment of the ongoing theta oscillations and benefitted performance, compared with

668   the arrhythmic train of pulses (Lakatos, Gross, & Thut, 2019; Riddle et al., 2020; Thut,

669   Schyns, & Gross, 2011; Thut, Veniero, et al., 2011).

670   In our study, the difference in theta activity observed between tasks suggests that its

671   function might go beyond the exertion of short-lasting top-down control over attentional

672   prioritization, but also encompasses the reformatting of the prioritized memoranda into

673   behavior-guiding representations. This is possible for the Implementation task, whereas

674   in the Memorization task the prioritized representations can only be used as a template

675   to guide the upcoming task (de Vries, Slagter, & Olivers, 2019; Olivers & Eimer, 2011;

676   Olivers, Peters, Houtkamp, & Roelfsema, 2011).

677   Therefore, the stronger theta activity in Implementation likely reflects the inherently more

678   extensive reformatting process of proceduralization, which we assume involves a theta-

679   driven binding between the stimulus and its corresponding motor plan (Combrisson et al.,

680   2017; Engel, Roelfsema, Fries, Brecht, & Singer, 1997; Verguts, 2017). The Memorization

681   task also requires the prioritization and the binding of stimulus and response, but this

682   would engage theta dynamics to a lesser extent, given the impossibility to activate a motor

683   plan.

684   Although strong conclusions cannot be made with respect to timing due to the temporal

685   smearing inherent to time-frequency analyses, attentional orienting and theta-mediated

686   binding seem to be occurring simultaneously. The temporal extents of the two clusters

687   are, in fact, largely overlapping. Therefore, our results hint at a parallel engagement of

688   the processes that underlie these frequencies.

689   *4.3 Motor preparation in Implementation is reflected in mu and beta suppression*

690   Previous fMRI studies showed that the proactive proceduralization of novel instructions

691   is accompanied by increased neural activity in pre-motor areas, suggesting motor

692   preparation (Bourguignon et al., 2018; Hartstra et al., 2011, 2012; Muhle-Karbe et al.,

693   2017; Ruge & Wolfensteller, 2010). In current views, the recruitment of motor areas is

694   thought to boost instruction implementation by enabling mental simulation of the overt

695   application of the instructed mappings (Brass et al., 2017). Motor imagery has been

696   associated with suppression in mu and beta bands over motor cortices (Cheyne, 2013;

697   McFarland et al., 2000; Pfurtscheller et al., 2006; Pfurtscheller & Neuper, 1997; Pineda,

698   2005), which we therefore predicted to occur while the participant is preparing to

699   implement a specific motor plan, as opposed to the declarative maintenance of the

700   mapping. Moreover, the engagement of motor areas during implementation is consistent

701   with the creation of a functional network optimized for the rapid and efficient execution of

702   the mappings.

703   In line with our hypothesis, we found these markers of motor preparation to be higher in

704   Implementation compared to Memorization, already during the CTI. While in both tasks

705   participants had to perform an overt motor response at the end of the trial, only during

706   Implementation they could proactively start preparing their response to the upcoming

707   target. This rules out the possibility that the observed differences reflect more general

708   mechanisms of unspecific motor energization, temporal estimation or target expectancy

709   (Nobre & Van Ede, 2018; Van Elswijk, Kleine, Overeem, & Stegeman, 2007; Wiener,

710 Parikh, Krakow, & Coslett, 2018). Overall, our results suggest that preparing to execute

711 novel mappings involves the activation of a specific motor plan corresponding to the

712 instructed response, to a much larger extent then the motor engagement observed in

713 Memorization.

714 Concerning the timing of the implementation-induced motor engagement, the temporal

715 extent of the significant cluster suggests a later onset with respect to alpha and theta

716 dynamics. Although strong conclusions cannot be drawn, based on this interpretation of

717 our permutation results and theoretical models such as Myers' (2017), we are inclined to

718 speculate that motor preparation is initiated following attentional selection of the relevant

719 mappings. From this perspective, theta would act as an overarching mechanism to bind

720 and control the task-optimized representations. Future studies should investigate the

721 exact timing properties and the interplay between these processes.

722   *4.4 Capacity limits of proceduralization*

723 As a corollary hypothesis, we predicted that the capacity limits of proceduralization

724 observed in behavioral studies (Liefooghe et al., 2012) would be reflected in stronger

725 proceduralization-related oscillatory features with fewer mappings. However, we did not

726 observe a significant interaction of Task and Load in none of our frequency bands of

727 interest. It is possible that our design was not powered enough to detect such effects.

728 Despite the not significant interaction, for exploratory purposes we looked at the effect of

729 Task separately for each Load. Interestingly, we observed task-related differences only

730 in Load 2. The interpretation of these results requires caution and can only be speculative

731 given the exploratory nature of these analyses. Yet, they could reflect that relevant

732 oscillations become crucial when in need to coordinate multiple bindings, but still within

733 capacity limitations. From this perspective, Load 4 would show no differences because

734 too many S-R mappings cannot be simultaneously recoded into action-oriented

735 representations (Liefooghe et al., 2012), and Load 1 would instead allow a more ballistic

736 implementation of the prepared motor plan, without the need to carefully coordinate

737 different competing procedural representations, as is the case in Load 2. These

738 exploratory results pave the way for future research investigating more accurately the

739 capacity limits of proceduralization: how they are overcome with extensive practice and

740 how they reflected in power modulations.

741

742 **5. Conclusions**

743 Our study shed light for the first time on the oscillatory dynamics associated with the

744 retrospective prioritization and proceduralization of novel instructions. We showed that

745 alpha-mediated mechanisms of attentional orienting are in place to prioritize the relevant

746 items, independently from the upcoming task demands. Conversely, other neural features

747 were sensitive to the task. The implementation of novel mappings, as opposed to their

748 declarative maintenance, is characterized by increased power in low frequencies and by

749 stronger suppression of mu and beta activity. The former is consistent with the purported

750 role of theta oscillations in cognitive control for the successful binding of stimulus and

751 response into a behavior-optimized procedure, and the latter to reflect motor preparation

752 of the instructed motor responses. Overall, our results support the idea that under optimal

753 task conditions, proceduralization can occur proactively in preparation for the upcoming

754 response execution demands.

755   Future research should investigate how proceduralization affects the underlying neural

756   representation of the instructed mapping, under the assumption that it is recoded from a

757   declarative to a procedural format, and how prefrontal regions mediate this reformatting

758   process. Moreover, future studies should explore whether capacity limits of

759   proceduralization (Liefooghe et al., 2012) are caused by concurrent activation of

760   interfering motor plans or intrinsic to the neural mechanisms supporting the recoding of

761   instructions into procedures, such as the theta-mediated binding.

762

770

771   **Data and code availability**

772   Data and code will be made available upon publication.

773

REFERENCES

Berger, B., Griesmayr, B., Minarik, T., Biel, A. L., Pinal, D., Sterr, A., & Sauseng, P. (2019). Dynamic regulation of interregional cortical communication by slow brain oscillations during working memory. *Nature Communications*, *10*(1), 1–11. https://doi.org/10.1038/s41467-019-12057-0

Bhandari, A., & Duncan, J. (2014). Goal neglect and knowledge chunking in the construction of novel behaviour. *Cognition*, *130*(1), 11–30. https://doi.org/10.1016/j.cognition.2013.08.013

Bonnefond, M., & Jensen, O. (2012). Alpha oscillations serve to protect working memory maintenance against anticipated distracters. *Current Biology*, *22*(20), 1969–1974. https://doi.org/10.1016/j.cub.2012.08.029

Bourguignon, N. J., Braem, S., Hartstra, E., De Houwer, J., & Brass, M. (2018). Encoding of Novel Verbal Instructions for Prospective Action in the Lateral Prefrontal Cortex: Evidence from Univariate and Multivariate Functional Magnetic Resonance Imaging Analysis. *Journal of Cognitive Neuroscience*, *26*(3), 1–15. https://doi.org/10.1162/jocn_a_01270

Brady, T. F., Konkle, T., Alvarez, G. A., & Oliva, A. (2013). Real-world objects are not represented as bound units: Independent forgetting of different object details from visual memory. *Journal of Experimental Psychology: General*, *142*(3), 791–808. https://doi.org/10.1037/a0029649

Brass, M., Liefooghe, B., Braem, S., & De Houwer, J. (2017). Following new task instructions: Evidence for a dissociation between knowing and doing. *Neuroscience*

796   *and Biobehavioral Reviews*, *81*(June), 16–28.

797   https://doi.org/10.1016/j.neubiorev.2017.02.012

798 Brass, M., Wenke, D., Spengler, S., & Waszak, F. (2009). Neural Correlates of

799   Overcoming Interference from Instructed and Implemented Stimulus-Response

800   Associations. *Journal of Neuroscience*, *29*(6), 1766–1772.

801   https://doi.org/10.1523/JNEUROSCI.5259-08.2009

802 Brodeur, M. B., Guérard, K., & Bouras, M. (2014). Bank of Standardized Stimuli (BOSS)

803   Phase II: 930 New Normative Photos. *PLoS ONE*, *9*(9), e106953.

804   https://doi.org/10.1371/journal.pone.0106953

805 Bundt, C., Bardi, L., Abrahamse, E. L., Brass, M., & Notebaert, W. (2015). It wasn't me!

806   Motor activation from irrelevant spatial information in the absence of a response.

807   *Frontiers in Human Neuroscience*, *9*(OCT).

808   https://doi.org/10.3389/fnhum.2015.00539

809 Capilla, A., Schoffelen, J.-M., Paterson, G., Thut, G., & Gross, J. (2014). Dissociated α-

810   Band Modulations in the Dorsal and Ventral Visual Pathways in Visuospatial

811   Attention and Perception. *Cerebral Cortex*, *24*(2), 550–561.

812   https://doi.org/10.1093/cercor/bhs343

813 Cavanagh, J. F., & Frank, M. J. (2014). Frontal theta as a mechanism for cognitive

814   control. *Trends in Cognitive Sciences*, *18*(8), 414–421.

815   https://doi.org/10.1016/j.tics.2014.04.012

816 Cheyne, D. O. (2013). MEG studies of sensorimotor rhythms: A review. *Experimental*

817   *Neurology*, *245*, 27–39. https://doi.org/10.1016/j.expneurol.2012.08.030

818   Cohen, M. X. (2014a). *Analyzing neural time series data: theory and practice*. MIT

819   Press.

820   Cohen, M. X. (2014b). Analyzing Neural Time Series Data.

821   Cohen, M. X., & Donner, T. H. (2013). Midfrontal conflict-related theta-band power

822   reflects neural oscillations that predict behavior. *Journal of Neurophysiology*,

823   *110*(12), 2752–2763. https://doi.org/10.1152/jn.00479.2013

824   Cole, M. W., Bagic, A., Kass, R., & Schneider, W. (2010). Prefrontal dynamics

825   underlying rapid instructed task learning reverse with practice. *Journal of*

826   *Neuroscience*, *30*(42), 14245–14254. https://doi.org/10.1523/JNEUROSCI.1662-

827   10.2010

828   Cole, M. W., Laurent, P., & Stocco, A. (2013). Rapid instructed task learning: A new

829   window into the human brain's unique capacity for flexible cognitive control.

830   *Cognitive, Affective, & Behavioral Neuroscience*, *13*(1), 1–22.

831   https://doi.org/10.3758/s13415-012-0125-7

832   Combrisson, E., Perrone-Bertolotti, M., Soto, J. L., Alamian, G., Kahane, P., Lachaux, J.

833   P., … Jerbi, K. (2017). From intentions to actions: Neural oscillations encode motor

834   processes through phase, amplitude and phase-amplitude coupling. *NeuroImage*,

835   *147*, 473–487. https://doi.org/10.1016/j.neuroimage.2016.11.042

836   Cooper, P. S., Karayanidis, F., McKewen, M., McLellan-Hall, S., Wong, A. S. W.,

837   Skippen, P., & Cavanagh, J. F. (2019). Frontal theta predicts specific cognitive

838   control-induced behavioural changes beyond general reaction time slowing.

839   *NeuroImage*, *189*(January), 130–140.

840   https://doi.org/10.1016/j.neuroimage.2019.01.022

841   de Vries, I. E. J., Slagter, H. A., & Olivers, C. N. L. (2019). Oscillatory Control over

842   Representational States in Working Memory. *Trends in Cognitive Sciences*.

843   https://doi.org/10.1016/j.tics.2019.11.006

844   de Vries, I. E. J., Van Driel, J., Karacaoglu, M., & Olivers, C. N. L. (2018). Priority

845   Switches in Visual Working Memory are Supported by Frontal Delta and Posterior

846   Alpha Interactions. *Cerebral Cortex*, *28*(11), 4090–4104.

847   https://doi.org/10.1093/cercor/bhy223

848   de Vries, I. E. J., van Driel, J., & Olivers, C. N. L. (2019a). Decoding the status of

849   working memory representations in preparation of visual selection. *NeuroImage*,

850   *191*, 549–559. https://doi.org/10.1016/j.neuroimage.2019.02.069

851   de Vries, I. E. J., van Driel, J., & Olivers, C. N. L. (2019b). Decoding the status of

852   working memory representations in preparation of visual selection. *NeuroImage*,

853   *191*, 549–559. https://doi.org/10.1016/J.NEUROIMAGE.2019.02.069

854   Delorme, A., & Makeig, S. (2004). EEGLAB : an open source toolbox for analysis of

855   single-trial EEG dynamics including independent component analysis. *Journal of*

856   *Neuroscience Methods*, *134*, 9–21. https://doi.org/10.1016/j.jneumeth.2003.10.009

857   Demanet, J., Liefooghe, B., Hartstra, E., Wenke, D., De Houwer, J., & Brass, M. (2016).

858   There is more into 'doing' than 'knowing': The function of the right inferior frontal

859   sulcus is specific for implementing versus memorising verbal instructions.

860   *NeuroImage*, *141*, 350–356. https://doi.org/10.1016/j.neuroimage.2016.07.059

861   Dumontheil, I., Thompson, R., & Duncan, J. (2011). Assembly and use of new task rules

862   in fronto-parietal cortex. *Journal of Cognitive Neuroscience*, *23*(1), 168–182.

863   https://doi.org/10.1162/jocn.2010.21439

864   Duncan, J., Emslie, H., Williams, P., Johnson, R., & Freer, C. (1996). Intelligence and

865   the Frontal Lobe: The Organization of Goal-Directed Behavior. *Cognitive*

866   *Psychology*, *30*(3), 257–303. https://doi.org/10.1006/COGP.1996.0008

867   Engel, A. K., Roelfsema, P. R., Fries, P., Brecht, M., & Singer, W. (1997). Role of the

868   temporal domain for response selection and perceptual binding. *Cerebral Cortex*,

869   *7*(6), 571–582. https://doi.org/10.1093/cercor/7.6.571

870   Everaert, T., Theeuwes, M., Liefooghe, B., & De Houwer, J. (2014). Automatic motor

871   activation by mere instruction. *Cognitive, Affective and Behavioral Neuroscience*,

872   *14*(4), 1300–1309. https://doi.org/10.3758/s13415-014-0294-7

873   Formica, S., González-García, C., & Brass, M. (2020). The effects of declaratively

874   maintaining and proactively proceduralizing novel stimulus-response mappings.

875   *Cognition*, *201*, 104295. https://doi.org/10.1016/j.cognition.2020.104295

876   Fries, P. (2005). A mechanism for cognitive dynamics: neuronal communication through

877   neuronal coherence. *Trends in Cognitive Sciences*, *9*(10), 474–480.

878   https://doi.org/10.1016/J.TICS.2005.08.011

879   Fries, P. (2015, October 7). Rhythms for Cognition: Communication through Coherence.

880   *Neuron*. Cell Press. https://doi.org/10.1016/j.neuron.2015.09.034

881   Fukuda, K., Mance, I., & Vogel, E. K. (2015). α power modulation and event-related

882   slow wave provide dissociable correlates of visual working memory. *Journal of*

883   *Neuroscience*, *35*(41), 14009–14016. https://doi.org/10.1523/JNEUROSCI.5003-

884   14.2015

885   González-García, C., Arco, J. E., Palenciano, A. F., Ramírez, J., & Ruz, M. (2017).

886   Encoding, preparation and implementation of novel complex verbal instructions.

887   *NeuroImage*, *148*(November 2016), 264–273.

888   https://doi.org/10.1016/j.neuroimage.2017.01.037

889   González-García, C., Formica, S., Liefooghe, B., & Brass, M. (2020). Attentional

890   prioritization reconfigures novel instructions into action-oriented task sets.

891   *Cognition*, *194*, 104059. https://doi.org/10.1016/j.cognition.2019.104059

892   González-García, C., Formica, S., Wisniewski, D., & Brass, M. (2019). Frontoparietal

893   action-oriented codes support novel task set implementation. *BioRxiv*, 830067.

894   https://doi.org/10.1101/830067

895   Gould, I. C., Rushworth, M. F., & Nobre, A. C. (2011). Indexing the graded allocation of

896   visuospatial attention using anticipatory alpha oscillations. *Journal of*

897   *Neurophysiology*, *105*(3), 1318–1326. https://doi.org/10.1152/jn.00653.2010

898   Goyal, A., Miller, J., Qasim, S., Watrous, A. J., Stein, J. M., Inman, C. S., … Jacobs, J.

899   (2020). Functionally distinct high and low theta oscillations in the human

900   hippocampus. *BioRxiv*, 498055. https://doi.org/10.1101/498055

901   Griffin, G., Holub, A., & Perona, P. (2007). Caltech-256 Object Category Dataset.

902   Retrieved from https://authors.library.caltech.edu/7694/

903   Groppe, D. M., Makeig, S., & Kutas, M. (2009). Identifying reliable independent

904   components via split-half comparisons. *NeuroImage*, *45*(4), 1199–1211.

905   https://doi.org/10.1016/j.neuroimage.2008.12.038

906   Haller, M., Donoghue, T., Peterson, E., Varma, P., Sebastian, P., Gao, R., … Voytek, B.

907   (2018). Parameterizing neural power spectra. *BioRxiv*, 299859.

908   https://doi.org/10.1101/299859

909   Hari, R., & Salmelin, R. (1997, January 1). Human cortical oscillations: A neuromagnetic

910   view through the skull. *Trends in Neurosciences*. https://doi.org/10.1016/S0166-

911   2236(96)10065-5

912   Hartstra, E., Kühn, S., Verguts, T., & Brass, M. (2011). The implementation of verbal

913   instructions: An fMRI study. *Human Brain Mapping*, *32*(11), 1811–1824.

914   https://doi.org/10.1002/hbm.21152

915   Hartstra, E., Waszak, F., & Brass, M. (2012). The implementation of verbal instructions:

916   Dissociating motor preparation from the formation of stimulus-response

917   associations. *NeuroImage*, *63*(3), 1143–1153.

918   https://doi.org/10.1016/j.neuroimage.2012.08.003

919   Itthipuripat, S., Wessel, J. R., & Aron, A. R. (2013). Frontal theta is a signature of

920   successful working memory manipulation. *Experimental Brain Research*, *224*(2),

921   255–262. https://doi.org/10.1007/s00221-012-3305-3

922   Jasp Team. (2019). JASP (Version 0.11.1)[Computer software]. Retrieved from

923   https://jasp-stats.org/

924 Jensen, O. (2002). Oscillations in the Alpha Band (9-12 Hz) Increase with Memory Load

925   during Retention in a Short-term Memory Task. *Cerebral Cortex*, *12*(8), 877–882.

926   https://doi.org/10.1093/cercor/12.8.877

927 Jensen, O., & Mazaheri, A. (2010). Shaping Functional Architecture by Oscillatory Alpha

928   Activity: Gating by Inhibition. *Frontiers in Human Neuroscience*, *4*(November), 1–8.

929   https://doi.org/10.3389/fnhum.2010.00186

930 Klem, G. H., Lüders, H. O., Jasper, H. H., & Elger, C. (1999). The ten-twenty electrode

931   system of the International Federation. The International Federation of Clinical

932   Neurophysiology. *Electroencephalography and Clinical Neurophysiology.*

933   *Supplement*, *52*, 3–6.

934 Klimesch, W., Sauseng, P., & Hanslmayr, S. (2007). EEG alpha oscillations: The

935   inhibition–timing hypothesis. *Brain Research Reviews*, *53*(1), 63–88.

936   https://doi.org/10.1016/J.BRAINRESREV.2006.06.003

937 Konkle, T., Brady, T. F., Alvarez, G. A., & Oliva, A. (2010). Conceptual distinctiveness

938   supports detailed visual long-term memory for real-world objects. *Journal of*

939   *Experimental Psychology: General*, *139*(3), 558–578.

940   https://doi.org/10.1037/a0019165

941 Lakatos, P., Gross, J., & Thut, G. (2019, September 23). A New Unifying Account of the

942   Roles of Neuronal Entrainment. *Current Biology*. Cell Press.

943   https://doi.org/10.1016/j.cub.2019.07.075

944 Liefooghe, B., & De Houwer, J. (2017). Automatic effects of instructions do not require

945   the intention to execute these instructions. *Journal of Cognitive Psychology*, *30*(1),

946   108–121. https://doi.org/10.1080/20445911.2017.1365871

947   Liefooghe, B., Wenke, D., & De Houwer, J. (2012). Instruction-based task-rule

948   congruency effects. *Journal of Experimental Psychology: Learning, Memory, and*

949   *Cognition*, *38*(5), 1325–1335. https://doi.org/10.1037/a0028148

950   Lisman, J. E., & Jensen, O. (2013). The Theta-Gamma Neural Code. *Neuron*, *77*(6),

951   1002–1016. https://doi.org/10.1016/j.neuron.2013.03.007

952   Manza, P., Hau, C. L. V., & Leung, H.-C. (2014). Alpha Power Gates Relevant

953   Information during Working Memory Updating. *Journal of Neuroscience*, *34*(17),

954   5998–6002. https://doi.org/10.1523/JNEUROSCI.4641-13.2014

955   Marchesotti, S., Bassolino, M., Serino, A., Bleuler, H., & Blanke, O. (2016). Quantifying

956   the role of motor imagery in brain-machine interfaces. *Scientific Reports*, *6*(1),

957   24076. https://doi.org/10.1038/srep24076

958   Maris, E., & Oostenveld, R. (2007). Nonparametric statistical testing of EEG- and MEG-

959   data. *Journal of Neuroscience Methods*, *164*, 177–190.

960   https://doi.org/10.1016/j.jneumeth.2007.03.024

961   Mazaheri, A., van Schouwenburg, M. R., Dimitrijevic, A., Denys, D., Cools, R., &

962   Jensen, O. (2014). Region-specific modulations in oscillatory alpha activity serve to

963   facilitate processing in the visual and auditory modalities. *NeuroImage*, *87*, 356–

964   362. https://doi.org/10.1016/J.NEUROIMAGE.2013.10.052

965   McFarland, D. J., Miner, L. A., Vaughan, T. M., & Wolpaw, J. R. (2000). Mu and Beta

966   Rhythm Topographies During Motor Imagery and Actual Movements. *Brain*

967   *Topography*, *12*(3), 177–186. https://doi.org/10.1023/A:1023437823106

968   McLelland, D., & VanRullen, R. (2016). Theta-Gamma Coding Meets Communication-

969   through-Coherence: Neuronal Oscillatory Multiplexing Theories Reconciled. *PLoS*

970   *Computational Biology*, *12*(10), e1005162.

971   Meiran, N., Pereg, M., Kessler, Y., Cole, M. W., & Braver, T. S. (2015a). Reflexive

972   activation of newly instructed stimulus–response rules: evidence from lateralized

973   readiness potentials in no-go trials. *Cognitive, Affective, & Behavioral*

974   *Neuroscience*, *15*(2), 365–373. https://doi.org/10.3758/s13415-014-0321-8

975   Meiran, N., Pereg, M., Kessler, Y., Cole, M. W., & Braver, T. S. (2015b). The power of

976   instructions: Proactive configuration of stimulus–response translation. *Journal of*

977   *Experimental Psychology: Learning, Memory, and Cognition*, *41*(3), 768–786.

978   https://doi.org/10.1037/xlm0000063

979   Milner, B. (1963). Effects of Different Brain Lesions on Card Sorting: The Role of the

980   Frontal Lobes. *Archives of Neurology*, *9*(1), 90–100.

981   https://doi.org/10.1001/archneur.1963.00460070100010

982   Mok, R. M., Myers, N. E., Wallis, G., & Nobre, A. C. (2016). Behavioral and Neural

983   Markers of Flexible Attention over Working Memory in Aging. *Cerebral Cortex*,

984   *26*(4), 1831–1842. https://doi.org/10.1093/cercor/bhw011

985   Muhle-Karbe, P. S., Duncan, J., De Baene, W., Mitchell, D. J., & Brass, M. (2017).

986   Neural Coding for Instruction-Based Task Sets in Human Frontoparietal and Visual

987   Cortex. *Cerebral Cortex (New York, N.Y. : 1991)*, *27*(3), 1891–1905.

988   https://doi.org/10.1093/cercor/bhw032

989   Myers, N. E., Stokes, M. G., & Nobre, A. C. (2017). Prioritizing Information during

990   Working Memory: Beyond Sustained Internal Attention. *Trends in Cognitive*

991   *Sciences*, *21*(6), 449–461. https://doi.org/10.1016/j.tics.2017.03.010

992   Myers, N. E., Walther, L., Wallis, G., Stokes, M. G., & Nobre, A. C. (2015). Temporal

993   Dynamics of Attention during Encoding versus Maintenance of Working Memory:

994   Complementary Views from Event-related Potentials and Alpha-band Oscillations.

995   *Journal of Cognitive Neuroscience*, *27*(3), 492–508.

996   https://doi.org/10.1162/jocn_a_00727

997   Neuper, C., & Pfurtscheller, G. (2001). Event-related dynamics of cortical rhythms:

998   Frequency-specific features and functional correlates. *International Journal of*

999   *Psychophysiology*, *43*(1), 41–58. https://doi.org/10.1016/S0167-8760(01)00178-7

1000   Nobre, A. C., & Van Ede, F. (2018). Anticipated moments: Temporal structure in

1001   attention. *Nature Reviews Neuroscience*, *19*(1), 34–48.

1002   https://doi.org/10.1038/nrn.2017.141

1003   Olivers, C. N. L., & Eimer, M. (2011). On the difference between working memory and

1004   attentional set. *Neuropsychologia*, *49*(6), 1553–1558.

1005   https://doi.org/10.1016/j.neuropsychologia.2010.11.033

1006   Olivers, C. N. L., Peters, J., Houtkamp, R., & Roelfsema, P. R. (2011, July). Different

1007   states in visual working memory: When it guides attention and when it does not.

1008   *Trends in Cognitive Sciences*. https://doi.org/10.1016/j.tics.2011.05.004

1009   Onton, J., Delorme, A., & Makeig, S. (2005). Frontal midline EEG dynamics during

1010   working memory. *NeuroImage*, *27*(2), 341–356.

https://doi.org/10.1016/J.NEUROIMAGE.2005.04.014

Oostenveld, R., Fries, P., Maris, E., & Schoffelen, J.-M. (2010). FieldTrip: Open Source Software for Advanced Analysis of MEG, EEG, and Invasive Electrophysiological Data. *Computational Intelligence and Neuroscience*, *2011*. https://doi.org/10.1155/2011/156869

Palenciano, A. F., González-García, C., Arco, J. E., Pessoa, L., & Ruz, M. (2019). Representational organization of novel task sets during proactive encoding. *The Journal of Neuroscience*, 0725–19. https://doi.org/10.1523/jneurosci.0725-19.2019

Palenciano, A. F., González-García, C., Arco, J. E., & Ruz, M. (2019). Transient and Sustained Control Mechanisms Supporting Novel Instructed Behavior. *Cerebral Cortex*, *29*(9), 3948–3960. https://doi.org/10.1093/cercor/bhy273

Perrin, F., Pernier, J., Bertrand, O., & Echallier, J. F. (1989). Spherical splines for scalp potential and current density mapping. *Electroencephalography and Clinical Neurophysiology*, *72*(2), 184–187. https://doi.org/10.1016/0013-4694(89)90180-6

Pfurtscheller, G., Brunner, C., Schlögl, A., & Lopes da Silva, F. H. (2006). Mu rhythm (de)synchronization and EEG single-trial classification of different motor imagery tasks. *NeuroImage*, *31*(1), 153–159. https://doi.org/10.1016/J.NEUROIMAGE.2005.12.003

Pfurtscheller, G., & Neuper, C. (1997). Motor imagery activates primary sensorimotor area in humans. *Neuroscience Letters*, *239*(2–3), 65–68. https://doi.org/10.1016/S0304-3940(97)00889-6

1032   Pineda, J. A. (2005). The functional significance of mu rhythms: Translating 'seeing' and

1033   'hearing' into 'doing'. *Brain Research Reviews*, *50*(1), 57–68.

1034   https://doi.org/10.1016/j.brainresrev.2005.04.005

1035   Poch, C., Campo, P., & Barnes, G. R. (2014). Modulation of alpha and gamma

1036   oscillations related to retrospectively orienting attention within working memory.

1037   *European Journal of Neuroscience*, *40*(2), 2399–2405.

1038   https://doi.org/10.1111/ejn.12589

1039   Poch, C., Carretie, L., & Campo, P. (2017). A dual mechanism underlying alpha

1040   lateralization in attentional orienting to mental representation. *Biological*

1041   *Psychology*, *128*(March), 63–70. https://doi.org/10.1016/j.biopsycho.2017.07.015

1042   Poch, C., Valdivia, M., Capilla, A., Hinojosa, J. A., & Campo, P. (2018). Suppression of

1043   no-longer relevant information in Working Memory: An alpha-power related

1044   mechanism? *Biological Psychology*, *135*(February), 112–116.

1045   https://doi.org/10.1016/j.biopsycho.2018.03.009

1046   Popov, T., Popova, P., Harkotte, M., Awiszus, B., Rockstroh, B., & Miller, G. A. (2018).

1047   Cross-frequency interactions between frontal theta and posterior alpha control

1048   mechanisms foster working memory. *NeuroImage*, *181*(July), 728–733.

1049   https://doi.org/10.1016/j.neuroimage.2018.07.067

1050   Rhodes, E., Gaetz, W. C., Marsden, J., & Hall, S. D. (2018). Transient Alpha and Beta

1051   Synchrony Underlies Preparatory Recruitment of Directional Motor Networks.

1052   *Journal of Cognitive Neuroscience*, *30*(6), 867–875.

1053   https://doi.org/10.1162/jocn_a_01250

Riddle, J., Scimeca, J. M., Cellier, D., Dhanani, S., Esposito, M. D., Riddle, J., …

    Esposito, M. D. (2020). Causal Evidence for a Role of Theta and Alpha Oscillations

    in the Control of Working Memory Report Causal Evidence for a Role of Theta and

    Alpha Oscillations in the Control of Working Memory. *Current Biology*, 1–7.

    https://doi.org/10.1016/j.cub.2020.02.065

Rihs, T. A., Michel, C. M., & Thut, G. (2007). Mechanisms of selective inhibition in visual

    spatial attention are indexed by α-band EEG synchronization. *European Journal of*

    Neuroscience, *25*(2), 603–610. https://doi.org/10.1111/j.1460-9568.2007.05278.x

Rihs, T. A., Michel, C. M., & Thut, G. (2009). A bias for posterior α-band power

    suppression versus enhancement during shifting versus maintenance of spatial

    attention. *NeuroImage*, *44*(1), 190–199.

    https://doi.org/10.1016/j.neuroimage.2008.08.022

Rohenkohl, G., & Nobre, A. C. (2011). Alpha oscillations related to anticipatory attention

    follow temporal expectations. *Journal of Neuroscience*, *31*(40), 14076–14084.

    https://doi.org/10.1523/JNEUROSCI.3387-11.2011

Ruge, H., Schäfer, T. A., Zwosta, K., Mohr, H., & Wolfensteller, U. (2019). Neural

    representation of newly instructed rule identities during early implementation trials.

    ELife, *8*, 1–25. https://doi.org/10.7554/eLife.48293

Ruge, H., & Wolfensteller, U. (2010). Rapid formation of pragmatic rule representations

    in the human brain during instruction-based learning. *Cerebral Cortex*, *20*(7), 1656–

    1667. https://doi.org/10.1093/cercor/bhp228

Sassenhagen, J., & Draschkow, D. (2019). Cluster-based permutation tests of

1076   MEG/EEG data do not establish significance of effect latency or location.

1077   *Psychophysiology*, (August 2018), 1–8. https://doi.org/10.1111/psyp.13335

1078   Sauseng, P., Klimesch, W., Stadler, W., Schabus, M., Doppelmayr, M., Hanslmayr, S.,

1079   … Birbaumer, N. (2005). A shift of visual spatial attention is selectively associated

1080   with human EEG alpha activity. *European Journal of Neuroscience*, *22*(11), 2917–

1081   2926. https://doi.org/10.1111/j.1460-9568.2005.04482.x

1082   Schneider, D., Barth, A., & Wascher, E. (2017). On the contribution of motor planning to

1083   the retroactive cuing benefit in working memory: Evidence by mu and beta

1084   oscillatory activity in the EEG. *NeuroImage*, *162*(April), 73–85.

1085   https://doi.org/10.1016/j.neuroimage.2017.08.057

1086   Schneider, D., Mertes, C., & Wascher, E. (2016). The time course of visuo-spatial

1087   working memory updating revealed by a retro-cuing paradigm. *Scientific Reports*,

1088   *6*(1), 21442. https://doi.org/10.1038/srep21442

1089   Senoussi, M., Moreland, J. C., Busch, N. A., & Dugué, L. (2019). Attention explores

1090   space periodically at the theta frequency. *Journal of Vision*, *19*(5), 1–17.

1091   https://doi.org/10.1167/19.5.22

1092   Senoussi, M., Verbeke, P., Desender, K., De Loof, E., Talsma, D., Verguts, T., &

1093   Dunantlaan, H. (2020). Theta oscillations shift towards optimal frequency for

1094   cognitive control. *BioRxiv*, 2020.08.30.273706.

1095   https://doi.org/10.1101/2020.08.30.273706

1096   Souza, A. S., & Oberauer, K. (2016). In search of the focus of attention in working

1097   memory: 13 years of the retro-cue effect. *Attention, Perception, & Psychophysics*,

1098   *78*(7), 1839–1860. https://doi.org/10.3758/s13414-016-1108-5

1099   Thut, G., Nietzel, A., Brandt, S. A., & Pascual-Leone, A. (2006). Alpha-band

1100   electroencephalographic activity over occipital cortex indexes visuospatial attention

1101   bias and predicts visual target detection. *The Journal of Neuroscience : The Official*

1102   *Journal of the Society for Neuroscience*, *26*(37), 9494–9502.

1103   https://doi.org/10.1523/JNEUROSCI.0875-06.2006

1104   Thut, G., Schyns, P. G., & Gross, J. (2011). Entrainment of Perceptually Relevant Brain

1105   Oscillations by Non-Invasive Rhythmic Stimulation of the Human Brain. *Frontiers in*

1106   *Psychology*, *2*(JUL), 170. https://doi.org/10.3389/fpsyg.2011.00170

1107   Thut, G., Veniero, D., Romei, V., Miniussi, C., Schyns, P., & Gross, J. (2011). Rhythmic

1108   TMS causes local entrainment of natural oscillatory signatures. *Current Biology*,

1109   *21*(14), 1176–1185. https://doi.org/10.1016/j.cub.2011.05.049

1110   Tzagarakis, C., West, S., & Pellizzer, G. (2015). Brain oscillatory activity during motor

1111   preparation: Effect of directional uncertainty on beta, but not alpha, frequency band.

1112   *Frontiers in Neuroscience*, *9*(JUN), 1–13. https://doi.org/10.3389/fnins.2015.00246

1113   Van Diepen, R., Foxe, J. J., & Mazaheri, A. (2019). The functional role of alpha-band

1114   activity in attentional processing: The current zeitgeist and future outlook. *Current*

1115   *Opinion in Psychology*. https://doi.org/10.1016/J.COPSYC.2019.03.015

1116   van Dijk, H., Schoffelen, J.-M., Oostenveld, R., & Jensen, O. (2008). Prestimulus

1117   oscillatory activity in the alpha band predicts visual discrimination ability. *The*

1118   *Journal of Neuroscience : The Official Journal of the Society for Neuroscience*,

1119   *28*(8), 1816–1823. https://doi.org/10.1523/JNEUROSCI.1853-07.2008

1120 van Ede, F. (2017). Mnemonic and attentional roles for states of attenuated alpha

1121   oscillations in perceptual working memory: A review. *European Journal of*

1122   *Neuroscience*, 1–7. https://doi.org/10.1111/ejn.13759

1123 van Ede, F. (2020). Visual working memory and action: Functional links and bi-

1124   directional influences. *Visual Cognition*, 1–13.

1125   https://doi.org/10.1080/13506285.2020.1759744

1126 van Ede, F., Chekroud, S. R., Stokes, M. G., & Nobre, A. C. (2019a). Concurrent visual

1127   and motor selection during visual working memory guided action. *Nature*

1128   *Neuroscience*, *22*(3), 477–483. https://doi.org/10.1038/s41593-018-0335-6

1129 van Ede, F., Chekroud, S. R., Stokes, M. G., & Nobre, A. C. (2019b). Concurrent visual

1130   and motor selection during visual working memory guided action. *Nature*

1131   *Neuroscience*, *22*(3), 477–483. https://doi.org/10.1038/s41593-018-0335-6

1132 Van Elswijk, G., Kleine, B. U., Overeem, S., & Stegeman, D. F. (2007). Expectancy

1133   induces dynamic modulation of corticospinal excitability. *Journal of Cognitive*

1134   *Neuroscience*, *19*(1), 121–131. https://doi.org/10.1162/jocn.2007.19.1.121

1135 Verbeke, P., & Verguts, T. (2019). Learning to synchronize: How biological agents can

1136   couple neural task modules for dealing with the stability-plasticity dilemma. *PLOS*

1137   *Computational Biology*, *15*(8), e1006604.

1138   https://doi.org/10.1371/journal.pcbi.1006604

1139 Verguts, T. (2017). Binding by random bursts: A computational model of cognitive

1140   control. *Journal of Cognitive Neuroscience*. https://doi.org/10.1162/jocn

1141   Wallis, G., Stokes, M., Cousijn, H., Woolrich, M., & Nobre, A. C. (2015). Frontoparietal

1142   and Cingulo-opercular Networks Play Dissociable Roles in Control of Working

1143   Memory. *Journal of Cognitive Neuroscience*, *27*(10), 2019–2034.

1144   https://doi.org/10.1162/jocn_a_00838

1145   Walter, W. G., Cooper, R., Aldridge, V. J., McCallum, W. C., & Winter, A. L. (1964).

1146   Contingent negative variation : An electric sign of sensori-motor association and

1147   expectancy in the human brain. *Nature*, *203*(4943), 380–384.

1148   https://doi.org/10.1038/203380a0

1149   Wenke, D., Gaschler, R., Nattkemper, D., & Frensch, P. A. (2009). Strategic influences

1150   on implementing instructions for future actions. *Psychological Research*

1151   *Psychologische Forschung*, *73*(4), 587–601. https://doi.org/10.1007/s00426-009-

1152   0239-x

1153   Wiener, M., Parikh, A., Krakow, A., & Coslett, H. B. (2018). An intrinsic role of beta

1154   oscillations in memory for time estimation. *Scientific Reports*, *8*(1), 1–17.

1155   https://doi.org/10.1038/s41598-018-26385-6

1156   Wolff, M. J., Ding, J., Myers, N. E., & Stokes, M. G. (2015). Revealing hidden states in

1157   visual working memory using electroencephalography. *Frontiers in Systems*

1158   *Neuroscience*, *9*(September), 1–12. https://doi.org/10.3389/fnsys.2015.00123

1159   Wolff, M. J., Jochim, J., Akyürek, E. G., & Stokes, M. G. (2017). Dynamic hidden states

1160   underlying working-memory-guided behavior. *Nature Neuroscience*, *20*(6), 864–

1161   871. https://doi.org/10.1038/nn.4546

1162